의학박사 학위논문

Natural polyphenols antagonize the antimyeloma activity of proteasome inhibitor bortezomib by direct chemical interaction

프로테아좀 억제제 보르테조밉과 천연 폴리페놀의

직접 화학상호작용에 의한 길항작용

2013 년 2 월

서울대학교 대학원

의과대학 분자종양의학 전공

김 태 영

Natural polyphenols antagonize the antimyeloma activity of proteasome inhibitor bortezomib by direct chemical interaction

프로테아좀 억제제 보르테조밉과 천연 폴리페놀의
직접 화학상호작용에 의한 길항작용

지도교수 이 동 순
이 논문을 의학박사 학위논문으로 제출함.
2012년 10월

서울대학교 대학원
의과대학 분자종양의학 전공
김 태 영

김태영의 의학박사 학위논문을 인준함.
2013년 2 월

위 원 장 _____
부위원장 _____
위 원 _____
위 원 _____
위 원 _____

Natural polyphenols antagonize the antimyeloma activity of proteasome inhibitor bortezomib by direct chemical interaction

by

Tae Young Kim

(Directed by Dong Soon Lee, M.D., Ph.D.)

A thesis submitted in partial fulfillment

of the requirements for the degree of

DOCTOR OF MEDICINE

Department of Molecular and Clinical Oncology

at Seoul National University College of Medicine

February, 2013

Approved by Thesis Committee:

Professor_____**Chairman**

Professor_____**Vice Chairman**

Professor_____

Professor_____

Professor_____

Abstract

Tae Young Kim
Department of Molecular and Clinical Oncology
The Graduate School
Seoul National University

Bortezomib is a therapeutic proteasome inhibitor with antimyeloma activity and polyphenols are well known compounds exerting antiproliferative effects against tumors. We attempted cotreatment of myeloma cells with bortezomib and polyphenols, anticipating a synergistic effect. However, the anticancer activity of bortezomib was blocked by the polyphenols. The structural features of the polyphenols correlated strikingly with their antagonistic effect; in particular, the presence or absence of a vicinal diol moiety was the key element for effective blockage of the anticancer function of bortezomib. We infer that the vicinal diols in the polyphenols interact with the boronic acid of bortezomib and convert the active triangular boronic acid of bortezomib to an inactive tetrahedral boronate, which abolishes the antimyeloma activity of bortezomib. We confirmed this hypothesis by ^{11}B NMR spectroscopy and an *in vitro* assay on myeloma cell lines and primary myeloma cells from patients. Based on these findings, restriction of the intake of natural polyphenols in foods or vitamin supplements during bortezomib treatment in multiple myeloma patients should be considered.

Key Words: bortezomib, polyphenols, multiple myeloma, drug-drug interaction, vicinal diol

***Student Number*:** 2005-30677

List of Figures

List of Tables

Contents

Introduction

Multiple myeloma (MM), associated with neoplastic plasma cell proliferation, is characterized by marked epidemiological, biological and clinical heterogeneity [1-3]. The bone marrow (BM) microenvironment, which comprises the extracellular matrix, bone marrow stromal cells (BMSCs) and MM cells, is also important for enhancing MM cell growth, survival, and migration. The binding of MM cells to BMSCs triggers the transcription and secretion of cytokines, including interleukin-6 (IL-6), insulin-like growth factor-1 (IGF-1), tumor necrosis factor-α (TNF-α), nuclear factor-κB (NF-κB), vascular endothelial growth factor (VEGF), and stromal cell-derived factor-1 (SDF-1) [4] (**Fig. 1**). As shown in Fig 1, MM cell growth is mediated via extracellular receptor kinase (ERK)/MAPK, survival via the Janus kinase (JAK)/signal transducer and activators of transcription (STAT), drug resistance via PI3-K/Akt, and migration via protein kinase C (PKC)–dependent signaling cascades. Signaling between these cytokines and MM cells as well as BMSCs is extensive and may lead to extramedullary disease and genetic alterations, including mutations of oncogenes (c-Myc, N-ras, and K-ras) and *p16* methylation have been implicated in the later stages of myeloma pathogenesis. In MM patients, chromosomal alterations are detected by conventional karyotyping and interphase fluorescence *in situ* hybridization (FISH) finds abnormalities in most cases [5]. Illegitimate recombination in MM involves *IgH* rearrangement at chromosome region 14q32, *FGFR3* and *MMSET* rearrangement (at 4p16.3), and *CCN D3*

rearrangement (at 6p21) [6]. Overexpression of several oncogenes, including *CCB D1* (at 11q13), *c-MAF* (at 16q23) [7], and *MAFB* (at 20q11) [8, 9] have also been reported. Despite high-dose stem-cell transplantation therapy and combination chemotherapy, MM has thus far remained as an incurable, relapsing, and refractory disease. Many new agents for treating MM are currently under investigation [10].

Proteasome is a very large 2.4 MDa subcellular organelle and is a multisubunit protein complex. It is also the site for the ATP-dependent degradation of ubiquitin-tagged proteins. Mis-folded intracellular proteins marked with a polyubiquitin chain by the E1-E2-E3 enzymatic cascade are targeted for degradation by proteasome (**Fig. 2**). Proteasome is composed of the 20S complex, which comprises α- and β-subunits, and two 19S regulatory complexes. The inner rings consist of seven β-subunits that form a central chamber – these contain the enzymatically active sites of the proteasome complex. Three (β1, β2 and β5) of the seven β-subunits perform the proteasome enzymatic activities, which have been characterized as chymotrytic-like, tryptic-like and caspase-like, respectively. Proteasomal degradation is a critical component of numerous cellular processes including cell cycle regulation [11], induction of the inflammatory response [12], and antigen presentation [13]. The notion that the malfunction of proteasomal degradation could either enhance the effect of oncoproteins or reduce the amount of suppressor proteins was first conceived when a number of oncogene and suppressor gene products were found to be targets of ubiquitylation. Therefore, it is

not surprising that aberrations of ubiquitylation have been linked to a wide range of pathologic states, including cancer.

Bortezomib (also known as PS-341: Velcade®), a proteasome inhibitor, is a well-known FDA (Food and Drug Administration)-approved anticancer agent with remarkable antiproliferative activity on MM cells and antitumor activity in a variety of *in vitro* and *in vivo* tumor models, either alone or in combination with other chemotherapeutic agents [14, 15]. The main mechanism underlying the action of bortezomib is the inhibition of NF-κB, and additional mechanisms include the down-regulation of several apoptosis inhibitors, the induction of caspase-dependent apoptosis, the release of intracellular reactive oxygen species (ROS), the inhibition of adhesion of MM cells to bone marrow stromal cells (BMSCs), and antiangiogenic activity [16, 17]. It was recently reported, though the striking myeloma killing effects of bortezomib, that MM patients could undergo neurotoxicity and pulmonary complications and acquire resistance to bortezomib during treatment, after which they do not respond to bortezomib [18-20].

Natural polyphenols, which are abundant in vegetables, grains, and fruits, are known to have antioxidant activity as efficient ROS scavengers. Moreover, they have potential antiproliferative activity on various tumor types [21, 22]. We screened a group of polyphenols for the measurement of their antiproliferative effects on hepatocellular carcinoma cells (data not shown) and selected 6 natural

polyphenols showing variable antiproliferative effects, as previously reported: quercetin dehydrate (QD) [23-26], rutin hydrate (RH) [27], (–)-epigallocatechin-3-gallate (EGCG) [28], caffeic acid (CA) [29], gallic acid (GA) [30], and tannic acid (TA) [31] (**Fig. 3**). QD could induce apoptosis and cell cycle arrest in several cancer cells by controlling intracellular proteins, protein kinase C, ErbB, β-catenin, $p27^{Kip1}$, or p53 [32-35]. RH, a derivative of QD, is reported to delay cellular oxidative stress and growth in the human hepatoma cell line HepG2 [36]. EGCG, the main active component of green tea, can kill the various human cancer cell lines by upregulating the Nrf2-ARE signaling pathway and inhibiting both STAT3 and NF-κB [37]. CA, GA, and TA are reported to have anti-tumor activity in certain tumor types: CA induces apoptosis in the HL-60 leukemic cell line [38], GA inhibits the proliferation of the MCF-7 breast cancer cell line [39], and TA inhibits skin tumorigenesis in CD-1 mice [40]. However, their mechanisms within the cells remain unclear.

Based on previous reports regarding combination therapies [41-43], we postulated that the antimyeloma activity of bortezomib would be enhanced by cotreatment with the polyphenols noted above. In order to determine the natural products that can synergistically enhance the potency of bortezomib, we cotreated MM cell lines and primary myeloma cells from patients with polyphenols and bortezomib. To ensure the generality of our study, we selected 3 representative MM cell lines with different genetic changes from among the available MM cell lines: U266, RPMI8226, and MC/CAR as shown in the Table 1 and Table 2.

Unexpectedly, polyphenols were observed to have antagonistic effects on bortezomib-induced apoptosis. In this study, we confirmed the direct chemical interaction and the resulting antagonism between bortezomib and naturally abundant polyphenols in MM cell lines and primary myeloma cells from patients. According to the FDA's prescription information on bortezomib, co-administration of Ketoconazol and Melphalan-Prednison can increase the exposure of botezomib. Also, concomitant administration of inhibitors or inducers of cytochrome P450 can cause drug interaction with bortezomib. The FDA recommends close monitoring of patients who are concomitantly receiving Ketaconazol and inhibitors or inducers of cytochrome P450 (http://www.fda.gov/cder/foi/label/2008/021602s015lbl.pdf). With regards to an interfering effect on bortezomib, antagonistic effects of vitamin C, Tiron, and quercetin [44-46] have been reported. However, the present study is the first systematic structural and mechanistic study on the direct chemical interactions of bortezomib. More importantly, the results of this study may provide guidelines to patients who are under bortezomib treatment and have ready access to polyphenols from their daily diets without knowledge of their potential antagonistic effects exerted via unexpected drug-drug interactions with bortezomib. Thus, we suggest that the intake of natural polyphenols should be avoided during treatment with bortezomib in patients with MM, in a manner similar to the avoidance of intake of vitamin K-containing foods for patients undergoing Warfarin therapy [47].

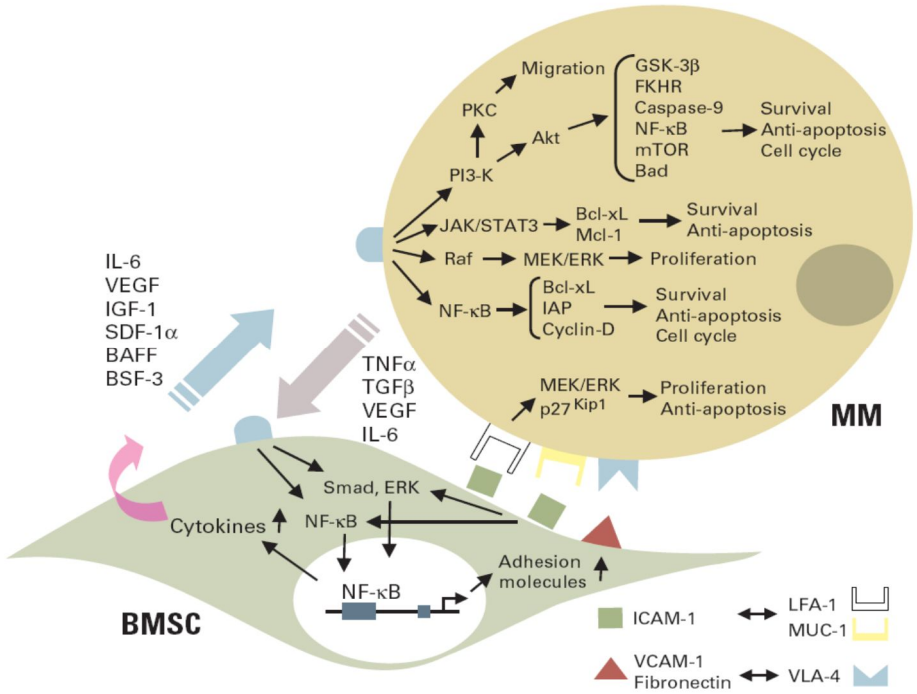

Hideshima, T., *et al*. 2005

Figure 1. The signaling cascades and molecular mechanisms triggered by interaction of multiple myeloma (MM) cells and bone marrow stromal cells (BMSCs). MM cell binding to BMSCs upregulates cytokine (IL-6, IGF-1, VEGF, SDF-1_) secretion from both BMSCs and MM cells. These cytokines subsequently activate three major signaling pathways (ERK, JAK/STAT3, and/or PI3-K/Akt) and their downstream targets including cytokines (IL-6, IGF-1, VEGF) and anti-apoptotic proteins (Bcl-xL, IAPs, Mcl-1) in MM cells. Adhesion mediated activation of nuclear factor kappa B (NF-κB) upregulates adhesion molecules (ICAM-1, VCAM-1) on both MM cells and BMSCs, further enhancing adhesion of MM cells to BMSCs and cytokine secretion (IL-6, interleukin-6; IGF-1, insulin-like growth factor-1; VEGF, vascular endothelial growth factor; SDF-1, stromal cell-derived factor-1; ERK, extracellular receptor kinase; JAK, janus kinase; STAT, signal transducer and activators of transcription; IAP, inhibitor of apoptosis; ICAM, intercellular adhesion molecule; VACM, vascular cell adhesion molecule; TNFα, tumor necrosis factor alpha; TGFβ, transforming growth factor beta).

A **B**

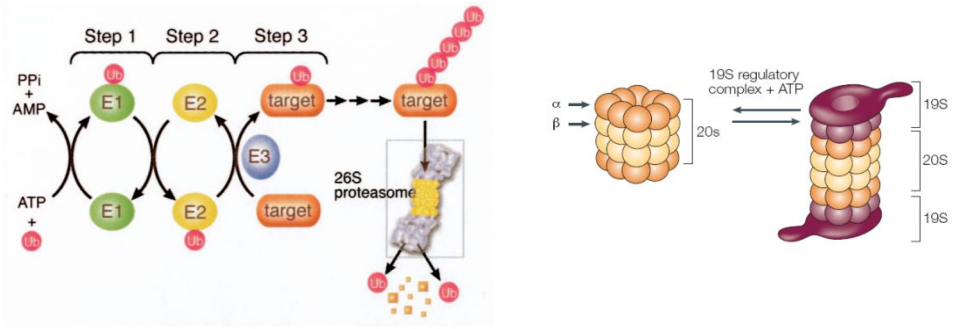

Mani, A., *et al* 2005 & Adams, J., 2004

Figure 2. The ubiquitin-proteasome pathway and the 26S proteasome structure. (A) Proteins marked with a polyubiquitin chain by the enzymatic cascade (E1, E2 and E3) are targeted for degradation by the proteasome. A ubiquitin-activating enzyme (E1) binds ubiquitin in an adenosine triphosphate (ATP)–dependent step. Ubiquitin is then transferred to a ubiquitin-conjugating enzyme or ubiquitin-carrier proteins (E2). A ubiquitin ligase (E3) helps transfer ubiquitin to the target substrate (PPI, pyrophosphate; AMP, adenosine monophosphate; Ub, ubiquitin). (B) A three-dimensional structure of the proteasome is composed of the 20S complex, and two 19S regulatory complexes. Together with ATP, these form the 26S proteasome.

Materials and methods

Reagents

Bortezomib (PS-341, Velcade®) was supplied by Millennium Pharmaceuticals Inc. (Cambridge, MA). Rutin hydrate (RH), quercetin dehydrate (QD), hydrocaffeic acid (CA), gallic acid (GA), and tannic acid (TA) were purchased from Sigma-Aldrich (St. Louis, MO). (–)-Epigallocatechin-3-gallate (EGCG) was purchased from WAKO (Osaka, Japan). Diphenylpicrylhydrazyl radical (DPPH) and flavonoids (F1: resokaempferol; F2: kaempferol; F3: molin; F4: isorhamnetin; F5: fisetin; F6: 2-(3,4-dihydroxyphenyl)-3,5,7-trihydroxy-4H-chromen-4-one; F7: myricetin; F8: 2-(3,4-dihydroxyphenyl)-7,8-dihydroxy-4H-chromen-4-one) were purchased from Sigma-Aldrich (St. Louis, MO). GA and TA were dissolved in 100% ethanol and the remaining polyphenols were dissolved in DMSO to a concentration of 100 mM at the stock solution and were diluted with growth medium to attain the desired concentration. Hydroethidine (HE), and 3, 3′-dihexyloxacarbocyanine iodide ($DiOC_6(3)$) were purchased from Invitrogen (Eugene, OR) and dissolved in DMSO.

Culture of the MM Cell lines and primary myeloma cells

The MC/CAR, RPMI8226 and U266 human MM cell lines were obtained from ATCC (American Type Culture Collection). The MC/CAR cell line was cultured in

Iscove's modified Dulbecco's medium (JBI, South Korea) with 25 mM HEPES containing 20% fetal bovine serum (FBS) (GIBCO, Grand Island, NY) and 100 units/mL of an antibiotic-antimycotic agent (GIBCO); the RPMI8226 and U266 cell lines were cultured in the RPMI1640 medium (JBI, South Korea) containing 10% FBS and 100 units/mL of an antibiotic-antimycotic agent at 37 ℃ in a 5% CO_2 humidified incubator. Primary myeloma cells from patients were cultured in the RPMI1640 medium containing 10% FBS, 100 units/mL of an antibiotic-antimycotic agent, 10 mM HEPES, 1 mM sodium pyruvate, 4.5 g/L glucose, and 0.05 mM 2-mercaptoethanol at 37 ℃ in a 5% CO_2 humidified incubator.

MM cell line characterization by fluorescence *in situ* hybridization (FISH)

Metaphase chromosomes were prepared from cells arrested in metaphase with 0.2 μg/ml colcemid (GIBCO-BRL) for 3 h and harvested according to the standard method. In brief, cells were treated with 5 ml of 0.25% trypsin till they dissociated and detached from the surface of culture flasks. Cells were then resuspended in 5 ml of fresh CO_2-independent medium supplemented with 10% FBS and immediately spun down by centrifugation at 1,200 rpm for 5 min (Beckman GS-6R). The supernatant was removed, and the cell pellet was treated with 5 ml of 75 mM KCl and gently resuspended in an additional 25 ml of the same concentration of KCl solution. The cell suspension was incubated at 20° C for 30 min and spun down at 1,200 rpm for 5 min. After the supernatant was removed, the cell pellet

was resuspended in 7 ml of a fixative (methanol–acetic acid 3:1) followed by centrifugation. The treatment with a fixative was repeated four times, and the cell pellet was resuspended in fixative in a final volume of 2 ml. These cells were then broken on glass slides by gravity to release chromosomes by dripping the cell mixture from a suitable distance above the slides. Chromosomes were stained by the conventional Giemsa stain method [48] and were observed at ×1000 magnification with immersion oil under a light microscope (Olympus IX50). About 500 mitotic figures from each single-cell clone were counted.

We performed FISH with *RB1* probe and D13S319 SpectrumOrange probe for detection of *Rb* deletion. For detection of the *IgH* rearrangement, LSI *IGH* Dual Color probe, LSI *IGH/CCND1* Dual Color probe, and LSI *IGH/BCL2* Dual Color probe were used. LSI *p58* (1p36)/LSI Telomere 1p/LSI 1q25 Microdeletion Probe Set were used for gain of 1q. All DNA FISH probes purchased from Vysis Inc. (Downers Grove, IL) and used according to the manufacturer's instructions.

MM cell line characterization by *p16* methylation-specific PCR and *ras* sequencing

For *p16* gene methylation-specific PCR, the genomic DNAs were modified by the bisulfite modification method according to the manufacturer's procedures (In2gene, South Korea). Primers for the detection of hypermethylation of *p16* gene, the

primers were used as previously described [49]. For *ras* mutation detection, the primers are listed in Table 2. The annealing temperatures of all primers were 58 °C.

Cell viability assay

For the cell viability assay, a CellTiter-Glo® Luminescent Cell Viability Assay (Promega, Madison, WI) was used in accordance with the manufacturer's instructions. Briefly, MM cell lines and the patient's primary cells (10,000–20,000 cells/well) were seeded in triplicate into 96-well plates. The cells were incubated with bortezomib (10 nM) and the desired concentrations of polyphenols to a final volume of 100 μL. After 48 h, 100 μL of CellTiter-Glo® reagent was added, followed by incubation for 10 min at room temperature. The luminescence was measured using a Wallac 1420 (PerkinElmer, Boston, MA).

In vitro 20S Proteasome activity assay

The MM cells (1×10^5 cells) were incubated for 3 h with bortezomib alone or with bortezomib and polyphenols, washed once with PBS, and resuspended in 160 μL of a cell lysis buffer as described previously [50]. After centrifugation, 50 μL of the cell supernatants were aliquoted into 96-well white-walled plates for measurement of the activity of 3 kinds of proteasomes (chemotrypsin-like, trypsin-like, and caspase-like). Proteasome-Glo™ Luminescent assay systems (Promega, Madison,

WI) were used according to the manufacturer's instructions in order to determine the proteasome activities.

Isolation of $CD138^+$ plasma cells from MM patients

Bone marrow (10 mL) from the MM patients was diluted with an equal volume of PBS and was layered gently on a Lymphoprep™ (AXIS-SHIELD, Oslo, Norway). The samples were centrifuged for 30 min at 2,000 rpm at room temperature. The interphase was carefully collected and washed twice with MACS buffer (1 × PBS containing 0.5% BSA and 2 mM EDTA). CD138 MicroBeads (Miltenyi Biotec, Auburn, CA) were added, and $CD138^+$ plasma cells were isolated according to the manufacturer's recommendations.

Immunoblotting Assay

Cells were washed with PBS once and lysed with RIPA buffer on ice. The cell lysates were normalized and 20 μg of total proteins were used for western blotting. The following antibodies were used: anti-PARP (Santa Cruz Biotechnology Inc., Santa Cruz, CA), anti-β-actin (Abcam Inc., Cambridge, MA), anti-caspase 8 (Cell Signaling, Danvers, MA), and anti-caspase 3/7 (cleaved form) (Cell Signaling). The following secondary antibodies were used: horseradish peroxidase-conjugated anti-rabbit IgG and anti-mouse IgG (Cell Signaling).

DPPH assay

We mixed 50 μL of diphenylpicrylhydrazyl radical (DPPH) (170 μM) in methanol and 100 μL of polyphenols (5 μM) in methanol in transparent 96-well plates. After 30 min, the absorbance at 515 nm was measured using an EL800 ELISA reader (BioTek, Winooski, VT)

Intracellular ROS detection

Drug-treated or untreated U266 cells were incubated with 10 μM of hydroethidine (HE) for 30 min at 37 °C prior to harvesting. The cells were then washed and resuspended with PBS. The intensity of fluorescence was measured by flow cytometry (BD Bioscience, San Jose, CA).

Apoptosis assessment by Annexin-V staining

Both drug-treated and untreated cells were washed with PBS and were stained with Annexin-V and propidium iodide (PI) according to the manufacturer's protocol (Roche, Mannheim, Germany). The percentage of apoptotic and necrotic cells was determined by FACSCalibur flow cytometry (BD Bioscience) using the Cell Quest software.

Analysis of mitochondrial membrane potential ($\Delta\Psi_m$)

RPMI8226 cells (at approximately 80% confluence in a 60-mm culture dish) were incubated with 40 nM 3,3′-dihexyloxacarbocynine iodide ($DiOC_6(3)$) in PBS at 37 °C for 20 min protecting from the light and were then analyzed by flow cytometry. The percentage of cells exhibiting a low level of $DiOC_6(3)$ uptake, reflecting the loss of mitochondrial membrane potential, was determined using a Becton Dickenson FACScan (San Jose, CA).

Nuclear Magnetic Resonance (NMR) Spectroscopy

The NMR spectra were recorded on a Bruker Biospin Avance 800 FT-NMR (Karlsruhe, Germany) (operated at 256.7 MHz for ^{11}B using H_3BO_2 as the internal standard). Methyl boronic acid and EGCG were dissolved in a DMSO:DPBS (1:3; pH 7.4) solution. ^{11}B NMR spectra of methyl boronic acid (0.5 mM) alone and of a mixture of methyl boronic acid (0.5 mM) and EGCG (200 mM, 400 equiv.) were recorded.

Results

Characterization of MM cell lines

We first characterized the 3 MM cell lines (U266, RPMI8226, and MC/CAR) used in this study. The U266 cell line had *p16* gene promoter hypermethylation without the *K-ras* and *N-ras* gene mutations. By fluorescence *in situ* hybridization (FISH), U266 showed a gain of the chromosome 1q, deletion of *Rb1*, and *IgH* rearrangement (Table 1). The RPMI8226 cell line showed hyperdiploidy, *p16* hypermethylation, and gain of 1q with a *K-ras* mutation at codon 12 (12 GGT→GCT), as shown in Table 2. MC/CAR had normal characters in the tested. In summary, the above 3 MM cell lines that had representative genetic changes were used for our *in vitro* study.

Table 1. Characterization of MM cell lines used in this study

	U266	RPMI8226	MC/CAR
FISH			
IgH break apart	*IgH* rearrangement	Normal	Normal
IgH / *CCND1*	*IgH* rearrangement	Tetrasomy 11	Normal
IgH / *BCL2*	*IgH* rearrangement	Tetrasomy 18	Normal
Rb1	*Rb1* deletion	Normal	Normal
gain of chromosome 1q	Trisomy 1q	Trisomy 1q and tetrasomy 1q	Normal
p16 methylation	methylation	methylation	unmethylation
Ras mutation	None	*K-ras* codon 12 heterozygous mutation	None

Table 2. Sequences of primers for the *K-ras* and *N-ras* sequencing

primer name	location	Sequence*
Kras_C12/13_F	*Kras* codon 12/13	5′-TCT GCA GTC AAC TGG AAT TT-3′
Kras_C12/13_R	*Kras* codon 12/13	5′-TGT TGG ATC ATA TTC GTC CA-3′
Kras_C61_F	*Kras* codon 61	5′-CTG TGT TTC TCC CTT CTC AG-3′
Kras_C61_R	*Kras* codon 61	5′-ATA CAC AAA GAA AGC CCT CC-3′
Nras_C12/13_F	*Nras* codon 12/13	5′-TAC TGG TTT CCA ACA GGT TC-3′
Nras_C12/13_R	*Nras* codon 12/13	5′-GGT GGG ATC ATA TTC ATC TA-3′
Nras_C61_F	*Nras* codon 61	5′-ACA AAC CAG ATA GGC AGA AA-3′
Nras_C61_R	*Nras* codon 61	5′-ATA CAC AGA GGA AGC CTT CG-3′

* The primers were used as previously described [49]

Polyphenols inhibited the growth of MM cells and induced apoptosis.

QD, CA, GA, EGCG, and TA induced cell death in a dose-dependent manner, showing remarkable antiproliferative effects on all of 3 MM cell lines, while RH showed a minimal antiproliferative effect (**Fig. 4A)**. QD, GA, EGCG, and TA showed a tendency of increased killing of RPMI8226 cells with time (24 hours, 48 hours, and 72 hours) but CA and RH did not show time dependent killing (**Fig. 4B**). The IC_{50} of QD, CA, GA, EGCG, and TA in U266 cells on day 2 was 50.5 μM, 61.9 μM, 23.3 μM, 28.0 μM, and 12.5 μM, respectively; 120.5 μM, 344.0 μM, 96.8 μM, 58.8 μM, and 11.0 μM, respectively, in RPMI8226 cells; and 24.2 μM, 99.2 μM, 43.6 μM, 72.9 μM, and 11.7 μM, respectively, in MC/CAR cells. By flow cytometry using Annexin-V and propidium iodide (PI), we also confirmed that the polyphenols efficiently killed the MM cells. In the flow cytometry study after 2 days of treatment with 100 μM each of RH, QD, CA, GA, EGCG, and TA, the percentage of Annexin-V-positive RPMI8226 cells was 5.3%, 63.5%, 10.0%, 12.5%, 31.5%, and 72.1%, respectively (**Fig. 4C**).

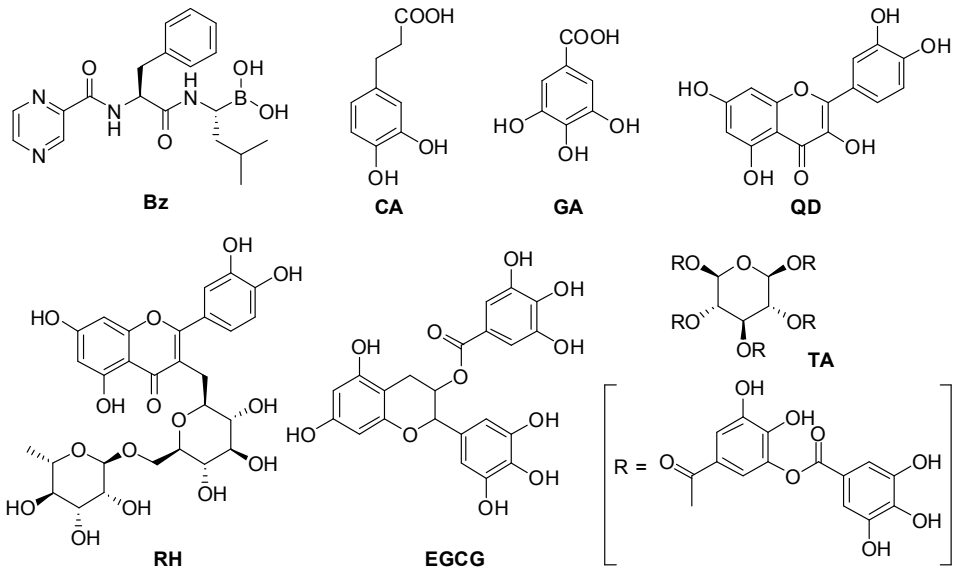

Figure 3. Chemical structures of bortezomib (Bz), caffeic acid (CA), gallic acid (GA), quercetin dehydrate (QD), rutin hydrate (RH), (–)-epigallocatechin-3-gallate (EGCG), and tannic acid (TA).

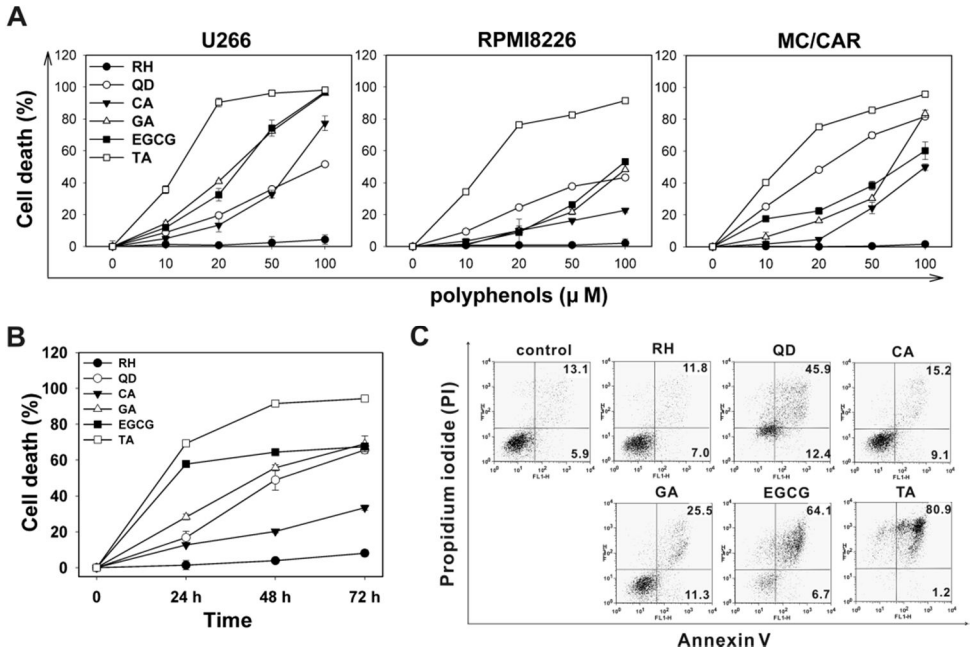

Figure 4. Antiproliferative effect of polyphenols on the MM cell lines. (A) MM cells were cultured with the indicated concentration of polyphenols for 48 h. Cell viability was assessed by the CellTiter-Glo® assay in 96-well plates, and the data represent mean (±SD) of triplicates. (B) Polyphenols could kill the RPMI8226 cells by a time-dependent manner (24, 48, and 72 h) at 100 μM concentration except RH. (C) Flow cytometric analysis by Annexin-V-FITC and propidium iodide (PI) staining was performed on RPMI8226 cells after 48 h treatment with 100 μM of each of the polyphenols.

Polyphenols blocked antiproliferative effect and proteasome inhibitory function of bortezomib in MM cell lines.

Upon bortezomib (10 nM) treatment in combination with various concentrations of polyphenols, the antiproliferative effect of the former was abolished even at low concentrations of polyphenols in all 3 genetically different MM cell lines (**Fig. 5A**). When RPMI8226 cells were treated with 100 μM of RH, 20 μM of QD, 20 μM of CA, 10 μM of GA, 10 μM of EGCG, and 2 μM of TA in the presence of bortezomib (10 nM), the percentage of revived cells was 13.8%, 70.4%, 82.6%, 75.8%, 89.0%, and 89.3%, respectively. RH showed a marginal inhibitory effect on bortezomib even at high concentration, i.e. 100 μM. The maximum blocking activity of QD and EGCG was observed at approximately 20 μM in all 3 MM cell lines. Both 20–70 μM of CA and 10–50 μM of GA showed maximum antagonism, depending on the cell lines. TA showed the strongest blocking effect even at low concentrations (2–5 μM). The antagonistic effect of polyphenols disappeared at high concentration, which resulted from their own cytotoxic effects. We quantified the antagonistic effect of each polyphenol on bortezomib in terms of the combination index (CI) computed using CalcuSyn software (Biosoft, Ferguson, MO, and Cambridge, UK) (**Table 3)**. The CI values of all polyphenols represented strong antagonism at 50% and 90% growth inhibition in the MM cell lines, except RH in U266 and RPMI8226 (because monotherapy with RH could not kill both cell lines) (see **Fig. 4B**). TA showed the most striking antagonism with a CI value of 6.70, 11.39, and 27.24 at ED_{90} in U266, RPMI8226, and MC/CAR, respectively, consistent with the previous results of a cell viability assay. Bortezomib is known

to predominantly inhibit the chymotrypsin-like and caspase-like protease function among 3 proteasome activities [51, 52]. Polyphenols abolished the inhibitory function of bortezomib (10 nM) on chymotrypsin-like and caspase-like activity of proteasome in a dose-dependent manner. The differences in killing activities between treatment of bortezomib alone and various combinations with polyphenols were found to be statistically significant by an unpaired student's *t*-test (Bz:RH, $P = 0.048$; Bz:QD, $P = 0.035$; Bz:CA, $P = 0.047$; Bz:GA, $P = 0.031$; Bz:EGCG, $P = 0.003$; Bz:TA, $P = 0.001$) (**Fig. 5B**).

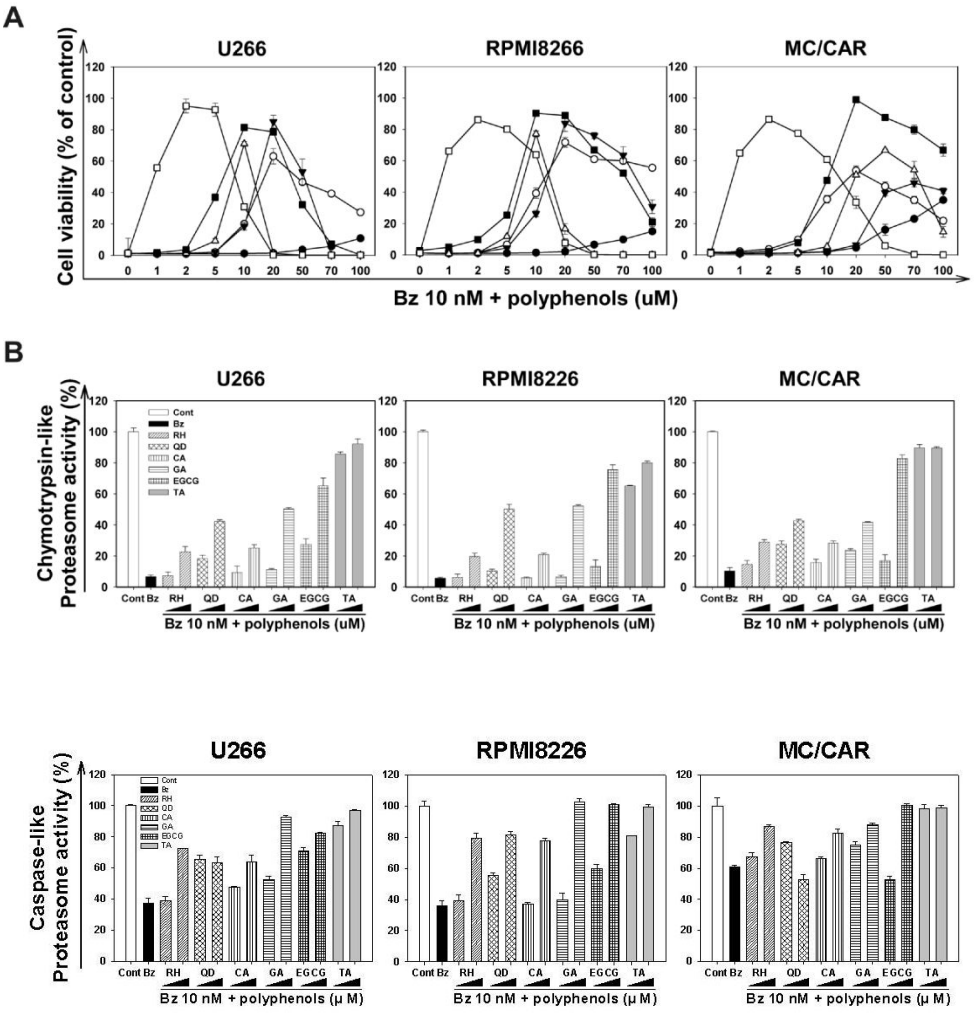
A
U266
RPMI8266
MC/CAR
Cell viability (% of control)
Bz 10 nM + polyphenols (uM)
B
U266
RPMI8226
MC/CAR
Chymotrypsin-like Proteasome activity (%)
Cont
Bz
RH
QD
CA
GA
EGCG
TA
Bz 10 nM + polyphenols (uM)
U266
RPMI8226
MC/CAR
Caspase-like Proteasome activity (%)
Bz 10 nM + polyphenols (μ M)

Figure 5. Polyphenols inhibited bortezomib-induced cell death and abrogated the proteasome inhibitory function of bortezomib in the MM cell lines. (A) After treatment of cells with bortezomib (10 nM) and with the indicated concentrations of RH (dark circles), QD (white circles), CA (dark triangles), GA (open triangles), EGCG (dark squares), and TA (open squires), cell viability was assessed by the CellTiter-Glo® assay in 96-well plates, and the data represent the mean ± SD (error bars) of triplicates. (B) MM cells were seeded onto 24-well plates with bortezomib alone (10 nM) or with bortezomib (10 nM) plus different concentrations of the indicated polyphenols (5 and 50 μM). At 3 h after drug treatment, the cells were harvested, and cell lysates were prepared as mentioned in Methods. Chymotrypsin-like and caspase-like proteasome activity was determined by the Proteasome-Glo™ assay. The data represent the mean ± SD (error bars) of triplicates ($P < 0.05$).

Table 3. Combination index (CI) values at 50% and 90% growth inhibition in the MM cell lines. The antagonistic activity of polyphenols against bortezomib was observed in the MM cell lines 48 h later after co-treatment of bortezomib and polyphenols. Combination index (CI) values were calculated using the CalcuSyn software according to the manufacturer's instruction. CI values < 1.0 indicate synergism, whereas CI values >1 indicate antagonism; 3.3 < CI < 10 indicates strong antagonism, and CI > 10 indicates very strong antagonism. Bz: bortezomib, RH: rutin hydrate, QD: quercetin dehydrate, CA: caffeic acid, GA: gallic acid, EGCG: (–)-epigallocatechin-3-gallate, and TA: tannic acid.

Cell line	Combination	Dose ratio	CI		parameters		
			ED_{50}	ED_{90}	IC_{50} (μM)	m	r
U266	Bz : RH	1:10,000	N/A	N/A	N/A	N/A	N/A
	Bz : QD	1:10,000	3.06	3.70	50.50	1.55	0.97
	Bz : CA	1:10,000	4.47	4.22	61.92	2.17	0.99
	Bz : GA	1:10,000	2.53	3.08	23.28	1.66	0.99
	Bz : EGCG	1:10,000	2.99	3.02	27.98	1.90	0.99
	Bz : TA	1:1,000	4.91	6.70	7.72	1.78	0.95
RPMI8226	Bz : RH	1:10,000	N/A	N/A	N/A	N/A	N/A
	Bz : QD	1:10,000	1.69	5.27	43.70	1.07	0.94
	Bz : CA	1:10,000	4.58	8.54	246.41	1.35	0.94
	Bz : GA	1:10,000	2.10	3.34	60.16	1.68	0.98
	Bz : EGCG	1:10,000	2.33	3.99	55.67	1.61	0.98
	Bz : TA	1:1,000	3.74	11.39	9.75	1.10	0.96
MC/CAR	Bz : RH	1:10,000	3.28	6.27	90.66	1.71	0.98
	Bz : QD	1:10,000	1.84	5.04	24.97	1.06	0.99
	Bz : CA	1:10,000	3.69	4.97	99.82	2.29	0.98
	Bz : GA	1:10,000	3.41	6.94	86.31	1.56	0.94
	Bz : EGCG	1:10,000	2.64	4.01	56.69	1.82	0.98
	Bz : TA	1:1,000	6.54	27.24	16.90	0.98	0.98

Polyphenols blocked bortezomib-induced apoptosis in MM cell lines.

Using Annexin-V and PI staining, the apoptotic and necrotic cell populations were measured by flow cytomery. The number of apoptotic cells was reduced when MM cells were cotreated with bortezomib and polyphenols at concentrations required for maximum blockage, as compared to treatment with bortezomib alone (**Fig. 6A**). By western blotting, we confirmed that the blocking effect of polyphenols was consistent with the previous results. Bortezomib-induced caspase/PARP cleavage was blocked by all 6 polyphenols (**Fig. 6B**). The activities of caspases-3, -8, and -9 as well as those of PARP, which are signature enzymes of cellular apoptotic events, were significantly reduced by cotreatment with bortezomib and polyphenols, as compared to monotherapy with bortezomib. Similar blocking effects were also observed on the mitochondrial membrane potential ($\Delta\Psi_m$) monitored using $DiOC_6(3)$ dye (**Fig. 6C**). Bortezomib-induced disruption of the mitochondrial membrane potential ($\Delta\Psi_m$) was also abolished by cotreatment with any of the 6 polyphenols. These results clearly support that polyphenols blocked bortezomib-induced apoptosis in MM cell lines.

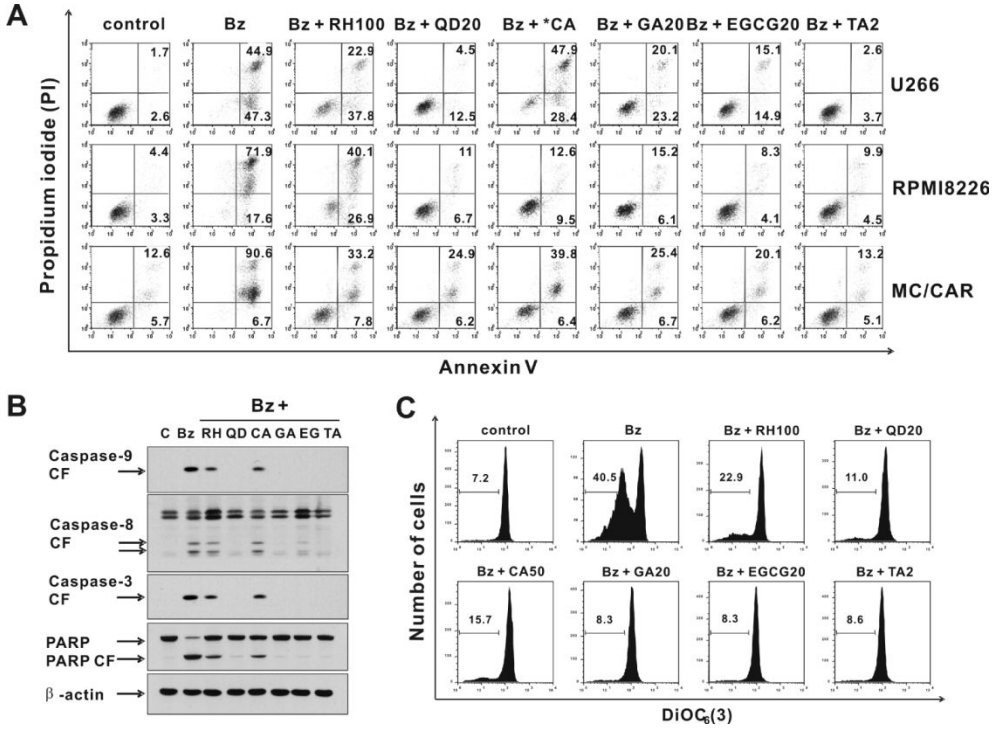
A
control
Bz
Bz + RH100
Bz + QD20
Bz + *CA
Bz + GA20
Bz + EGCG20
Bz + TA2
Propidium iodide (PI)
Annexin V
U266
RPMI8226
MC/CAR
1.7
2.6
44.9
47.3
22.9
37.8
4.5
12.5
47.9
28.4
20.1
23.2
15.1
14.9
2.6
3.7
4.4
3.3
71.9
17.6
40.1
26.9
11
6.7
12.6
9.5
15.2
6.1
8.3
4.1
9.9
4.5
12.6
5.7
90.6
6.7
33.2
7.8
24.9
6.2
39.8
6.4
25.4
6.7
20.1
6.2
13.2
5.1
B
Bz +
C Bz RH QD CA GA EG TA
Caspase-9 CF
Caspase-8 CF
Caspase-3 CF
PARP
PARP CF
β -actin
C
control
Bz
Bz + RH100
Bz + QD20
Bz + CA50
Bz + GA20
Bz + EGCG20
Bz + TA2
Number of cells
7.2
40.5
22.9
11.0
15.7
8.3
8.3
8.6
DiOC6(3)

Figure 6. Bortezomib-induced apoptosis was blocked by polyphenols in the MM cell lines. (A) MM cells were cultured for 48 h with bortezomib (10 nM) and the indicated concentration of each polyphenol except CA. The CA concentration was 20 μM in U266, 50 μM in RPMI8226, and 70 μM in MC/CAR depending on its maximum blocking activity according to the cell viability assay data. The cells were subjected to Annexin-V-FITC and propidium iodide (PI) staining to determine apoptosis by flow cytometry. (B) The RPMI8226 cells were cultured for 24 h with bortezomib (10 nM) and the indicated concentrations (μM) of polyphenols. Whole-cell lysates were subjected to western blotting using anti-caspase-3, -8, and -9 antibodies as well as anti-PARP antibody. The anti-β-actin antibody was used as the protein quantity control. CF: cleaved form. (C) RPMI8226 cells were cultured for 24 h with bortezomib (10 nM) alone or bortezomib (10 nM) plus the indicated concentrations (μM) of polyphenols. The mitochondrial membrane potentials ($\Delta\Psi_m$) were measured using 40 nM $DiOC_6(3)$.

The inhibitory effect of polyphenols on bortezomib was also observed in primary myeloma cells from patients.

To confirm the inhibitory effect of polyphenols on bortezomib in patients, we performed a cell viability assay using the primary plasma cells from 6 MM patients. MM cells enriched with CD138 microbeads were obtained from the patient's bone marrow aspirates. All 6 polyphenols demonstrated the different levels of blocking on the antiproliferative activity of bortezomib in the primary myeloma cells from 6 patients, which is consistent with the results obtained in the 3 genetically different MM cell lines (**Fig. 7**).

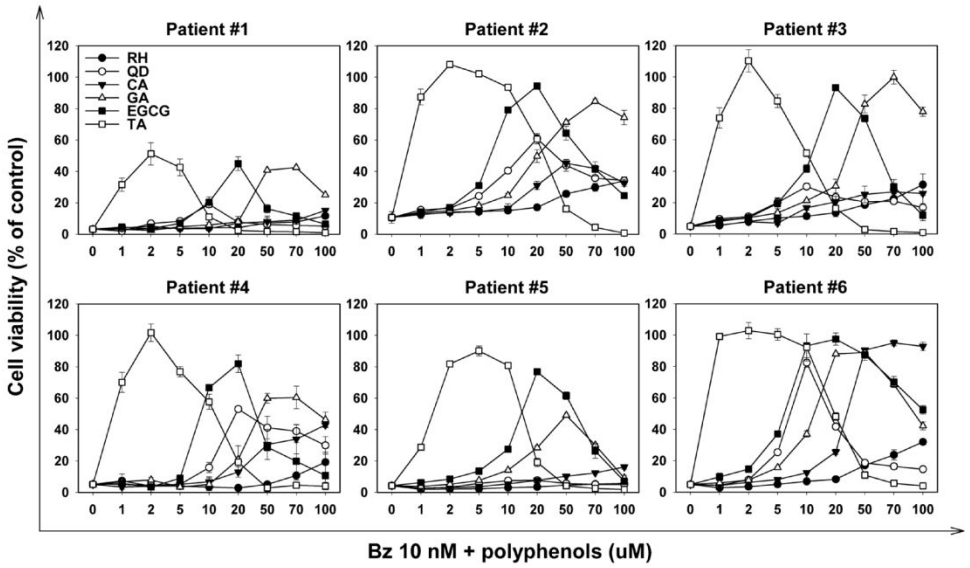

Figure 7. Inhibitory effects of polyphenols on bortezomib were observed in the primary myeloma cells from MM patients. $CD138^{+}$ myeloma cells were isolated from bone marrow aspirates of 6 MM patients using MACS CD138 MicroBeads. Cell survival was determined by the CellTiter-Glo® assay in 96-well culture plates. All experimental conditions were identical to those used for the experiment involving the cell lines.

Effect of polyphenols on bortezomib-induced intracellular ROS generation

To elucidate the inhibitory interaction between bortezomib and polyphenols, we measured the alteration of ROS generation induced by bortezomib in MM cells. Since most polyphenols serve as potent antioxidants intracellularly [22], we speculated that they could block bortezomib-induced apoptosis through efficient scavenging of bortezomib-induced ROS in MM cells. To quantify the ROS levels in MM cells, we introduced hydroethidine (HE) to measure the superoxide levels in live cells that had been treated with bortezomib and individual polyphenols. The maximum ROS level with HE was detected in the U266 cell line after incubation with bortezomib (10 nM) for 7 h (**Fig. 8A**). These results initially led us to conclude that the antagonistic effect of polyphenols is simply caused by efficient scavenging of the bortezomib-induced ROS, which triggers the apoptotic pathway. Therefore, we examined the antioxidant potential of all 6 polyphenols by a standard diphenylpicrylhydrazyl (DPPH) radical assay. The polyphenols tested in this study demonstrated an antioxidant potential similar to or higher than that of vitamin C (**Fig. 8B**). It was remarkable that the antioxidant activity of EGCG and TA was approximately 3- and 10-fold higher, respectively, than that of vitamin C. However, we noticed a discrepancy between the antioxidant potential of the polyphenols and the cellular ROS levels quantified using HE in the U266 cell line. If indeed efficient ROS scavenging by the polyphenols was the key element responsible for antagonism of bortezomib-induced cell death, the ROS level in the MM cells treated with bortezomib and TA would be the lowest given that the

antioxidant potential of TA is the strongest. However, there were no significant differences in the ROS levels in the U266 cells; further TA, RH, and CA efficiently decreased the ROS levels almost to that in the control. However, EGCG, QD, and GA failed to bring about a similar decrease in the ROS levels in the U266 cells. Based on this finding, we concluded that the antioxidant potential of the polyphenols does not have a direct correlation with the ROS level in the U266 cells as measured by HE. It is thus unlikely that ROS generation is the single major mechanism for bortezomib-induced cell death.

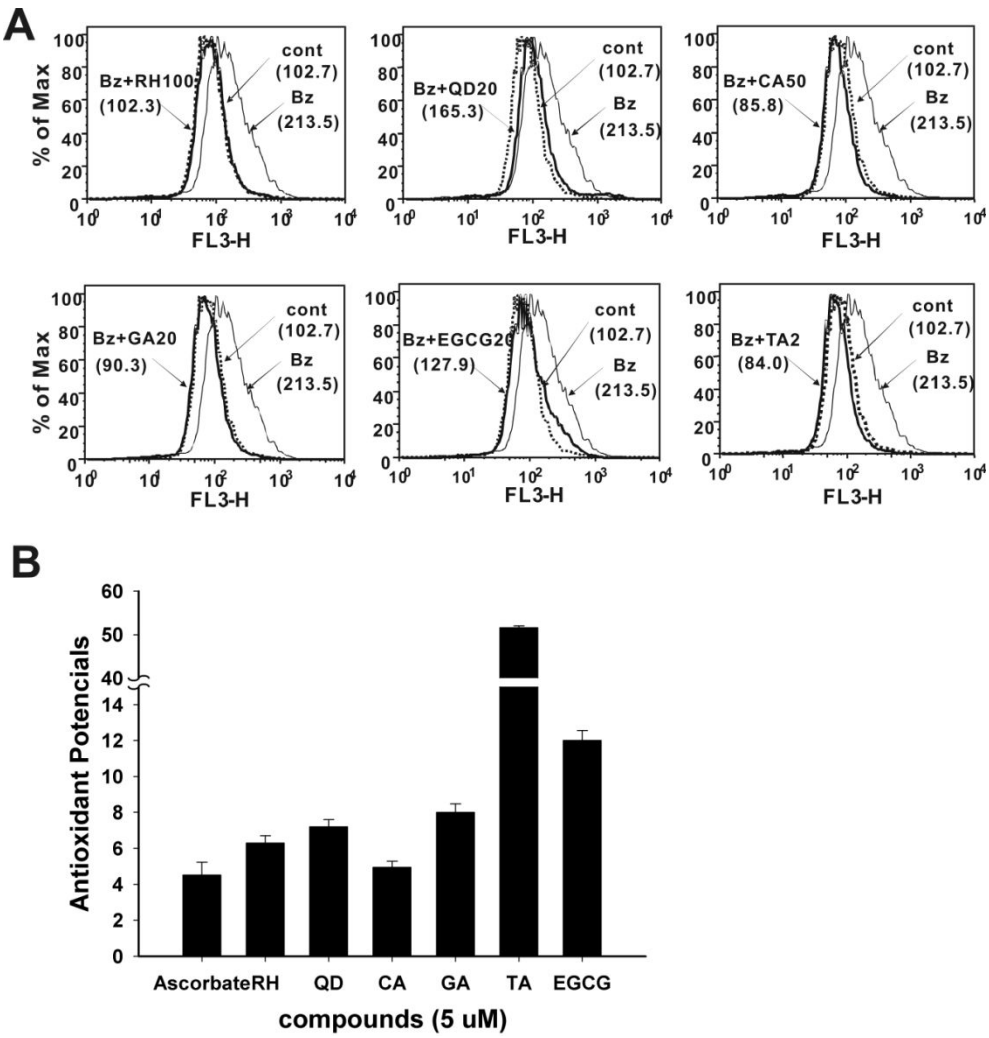
A
% of Max
Bz+RH100
(102.3)
cont
(102.7)
Bz
(213.5)
FL3-H
Bz+QD20
(165.3)
Bz+CA50
(85.8)
Bz+GA20
(90.3)
Bz+EGCG20
(127.9)
Bz+TA2
(84.0)

B
Antioxidant Potencials
AscorbateRH
QD
CA
GA
TA
EGCG
compounds (5 uM)

Figure 8. Effect of polyphenols on bortezomib-induced ROS generation. (A) *In vitro* superoxide generation by bortezomib itself or in combination with polyphenols. The U266 cells were exposed to the indicated treatment for 7 h. The varied levels of intracellular ROS generation were measured using the HE dye. The solid bold lines indicate the cells treated with bortezomib (Bz, 10 nM) plus polyphenols (μM); the solid lines indicate bortezomib-treated (10 nM) cells; and the bold dotted-lines indicate the control cells. (B) The antioxidant potentials of polyphenols in the DPPH assay. Polyphenols (5 μM) were mixed with DPPH (170 μM) in methanol, and the absorbance at 515 nm was measured using an ELISA reader.

Polyphenols blocked the activity of bortezomib by direct chemical interaction

Based on the above conclusion, we hypothesized that the structural features of polyphenols might induce their direct chemical interaction with bortezomib, and this could be the major cause of their antagonistic effect. To confirm the correlation between the structure of polyphenols and their bortezomib-blocking ability, we selected eight polyphenols (flavonoids) having an identical core structure but different positions and numbers of hydroxyl group substitutions (**Fig. 9A**). We performed a series of cell viability assays in the presence of bortezomib (10 nM) cotreated individually with each of the 8 polyphenols. As shown in **Fig. 9B**, an antagonistic rescues from bortezomib-induced apoptosis was observed in the case of F5~F8. The enhanced cell viability at a 20 μM concentration of F5~F8 had a significant correlation with the structural features of the flavonoids; that is, they all have vicinal diols. However, F1~F4 had no antagonistic effect on the antiproliferative activity of bortezomib and interestingly, they all have no vicinal diols. The treatment with 20 μM of F8 showed the most effective blockage among the 8 polyphenols, and the blockage of the antiproliferative effect was diminished at high dosage (>50 μM) of flavonoids owing to their own cytotoxicity. When we performed a DPPH assay on 8 polyphenols, the polyphenols with the vicinal diol moiety (F5~F8) showed similar antioxidant abilities and higher antioxidant abilities than those without the vicinal diol moiety (F1~F4). This would indicate that the ROS-scavenging activity is the key element responsible for the antagonistic effect of polyphenols. However, the ROS-scavenging potential of F3

at 20 μM is much higher than that of F5~F8 at 3.3 μM. If the ROS-scavenging ability is indeed the key element responsible for the antagonistic effect, we should have observed antagonistic cell viability rescue at a higher concentration of F1~F4; however, we did not observe revitalization of bortezomib-treated MM cells. An increase in the concentration of F3 from 4 μM to 20 μM raised its antioxidant potential but did not affect its bortezomib-blocking effect (**Fig. 9B, C**). Therefore, we concluded that the structural feature of polyphenols—and not their ROS-scavenging potential as antioxidants—is the major element responsible for their antagonistic effect on bortezomib-induced cell death.

To obtain clear evidence on the direct chemical interaction between bortezomib and polyphenol, the ^{11}B NMR spectrum of methyl boronic acid was recorded in the absence and presence of polyphenol, respectively. We chose EGCG as a representative polyphenol and methyl boronic acid as the substitute for bortezomib (**Fig. 9D**). The ^{11}B chemical shift of methyl boronic acid (0.5 mM) changed from 32.41 ppm, which is characteristic of the trigonal structure (sp^2) of boronic acid, in the absence of EGCG to 14.05 ppm, which is characteristic of tetrahedral structure (sp^3) of boronate, in the presence of EGCG (200 mM) [53, 54]. A large excess of EGCG (400-fold) was required for the direct chemical interaction to be detectable by ^{11}B NMR. In fact, the maximum antagonistic effect of EGCG was observed at 20 μM when the MM cells were treated with bortezomib (10 nM). This implies that efficient antagonism of the antiproliferative activity of bortezomib was achieved with a 2000-fold excess of EGCG. The ^{11}B NMR spectra provided a clear confirmation of the direct drug-drug interaction between bortezomib and

polyphenols, where a vicinal diol is required as the key structural feature for efficient chemical interaction with the boronic acid moiety of bortezomib.

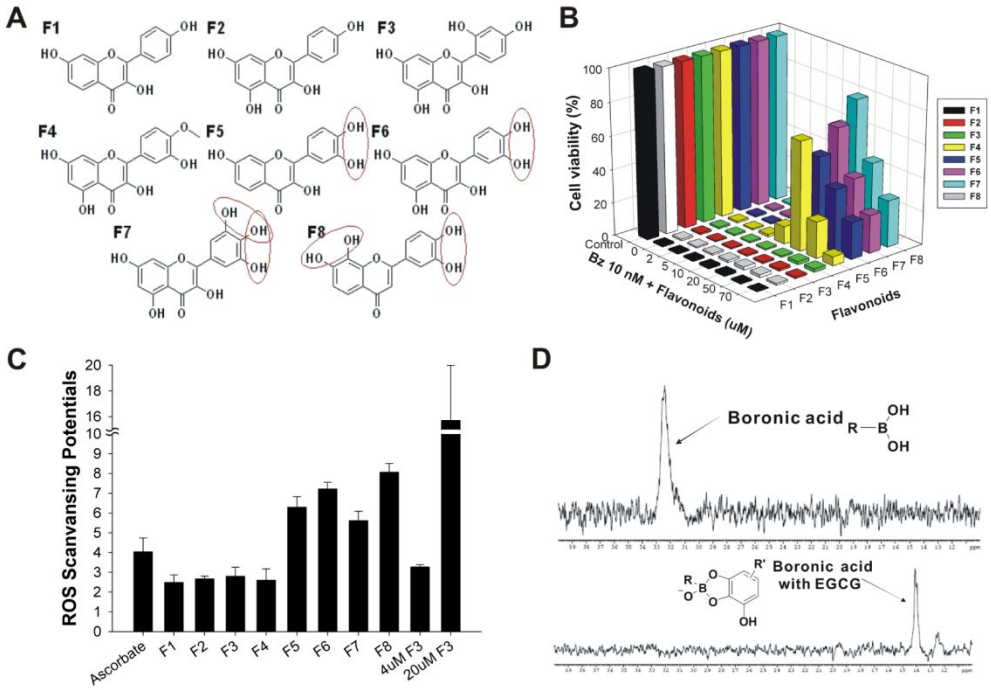
A
F1
F2
F3
F4
F5
F6
F7
F8
B
Cell viability (%)
100
80
60
40
20
0
Control
0
2
5
10
20
50
70
Bz 10 nM + Flavonoids (uM)
F1 F2 F3 F4 F5 F6 F7 F8
Flavonoids
C
ROS Scanvansing Potentials
20
18
16
10
9
8
7
6
5
4
3
2
1
0
Ascorbate
F1
F2
F3
F4
F5
F6
F7
F8
4uM F3
20uM F3
D
Boronic acid
R—B
OH
OH
R'
Boronic acid
with EGCG
OH

Figure 9. Direct chemical interaction between polyphenols and bortezomib. (A) The chemical structures of 8 polyphenols (F1~F8) having various number and positions of hydroxyl group substitutions. The vicinal hydroxyl group is indicated in the figure. (B) Cell viability assay data after co-treatment with bortezomib and various concentrations of the 8 polyphenols for 48 h in RPMI8226 cell line. (C) Antioxidant potentials of the 8 polyphenols at 3.3 μM in the DPPH assay. F3 at a high concentration (20 μM) showed a significantly high antioxidant potential. (D) ^{11}B NMR spectra of boronic acid in the absence and presence of EGCG. F1: resokaempferol; F2: kaempferol; F3: molin; F4: isorhamnetin; F5: fisetin; F6: 2-(3,4-dihydroxyphenyl)-3,5,7-trihydroxy-4H-chromen-4-one; F7: myricetin; F8: 2-(3,4-dihydroxyphenyl)-7,8-dihydroxy-4H-chromen-4-one.

In vitro study on the time duration of blocking effect of polyphenol

We attempted to assess the duration of the blocking effect of polyphenol on bortezomib-induced cell death by addition of polyphenols at a series of time intervals after treatment of 3 genetically different MM cell lines with bortezomib. MM cells were treated with 20 μM of EGCG or 2 μM of TA for 1–36 h after treatment with 10 nM of bortezomib (**Fig. 10A, B**). The blocking effect of EGCG or TA deteriorated in a time-dependent manner, and the antagonistic effect of polyphenols was not observed at 36 h after bortezomib treatment.

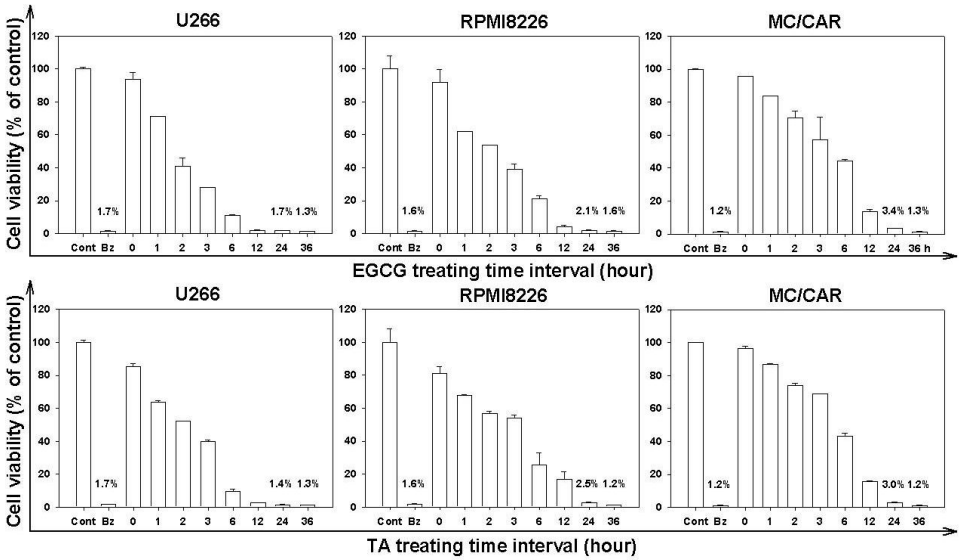

Figure 10. **The duration of the blocking activity of polyphenols after bortezomib treatment in the MM cell lines.**

The MM cells were treated with EGCG (A) or TA (B) for 1–36 h after bortezomib (10 nM) treatment, and cell viability was accessed. Cont: control, Bz: bortezomib, EGCG: (–)-epigallocatechin-3-gallate, and TA: tannic acid.

Discussion

At the early stage of our research, we suspected that the antioxidant function of polyphenols is mainly responsible for their antagonistic effects on bortezomib because polyphenols might efficiently scavenge the ROS, the generation of which is induced by bortezomib and which triggers the apoptotic pathway. To investigate this, we measured the ROS level in cells after the treatment with bortezomib alone or treatment with bortezomib and polyphenols. However, the antioxidant potential of the polyphenols showed no significant correlations with their antagonistic effects on bortezomib function. On the contrary, the structure of polyphenol appears to be the key factor responsible for their blocking effect on bortezomib. Therefore, we screened the antagonistic effects of a series of polyphenols having an identical core structure with various hydroxyl group substitution patterns on bortezomib-induced cell death (**Fig 9A**). Interestingly, the structural features of polyphenols showed striking correlations with their antagonistic effects, and in particular the presence or absence of vicinal diol moieties in the polyphenols was the key factor responsible for their blocking effects on the anticancer function of bortezomib. This observation is supported by the finding that the number of vicinal diols does not determine the antioxidant potential but significantly influences the antagonistic effect of polyphenols on bortezomib. Therefore, it was apparent that the anticancer activity of bortezomib can be blocked by direct chemical interaction of vicinal diols in polyphenols with the boronic acid moiety of bortezomib.

Regarding a mechanistic understanding of the antagonistic effect on bortezomib-induced cell death, we inferred that the vicinal diol in the polyphenols interacts with the boronic acid of bortezomib and converts the active triangular boronic acid (sp^2 character) of bortezomib to an inactive tetrahedral boronate (sp^3 character) through direct chemical interaction. The equilibrium of this conversion is controlled by the structure and concentration of polyphenols, and this conversion abolishes the antimyeloma activity of bortezomib. We confirmed this hypothesis on the drug-drug interaction of bortezomib with polyphenols through ^{11}B NMR spectroscopy.

Based on our results, we conclude that the antimyeloma activity of bortezomib can be blocked *in vitro* by polyphenols containing vicinal diols. Our study, i.e., an investigation of the chemical interactions between bortezomib and polyphenols is important because the latter are abundant in our daily diet. Furthermore, the consumption of polyphenols is expected to increase due to the increased use of dietary supplements and public health initiatives encouraging the consumption of more wine, herbs, fruits, and vegetables [52, 53]. Drug-food interactions, except for some interactions that affect drug absorption, have been largely overlooked by many clinicians. The concentration ratio of polyphenols to bortezomib ranges from 35 to 150 depending on the polyphenols with respect to exerting a blocking effect on bortezomib [55-57]. Plasma concentrations of polyphenols containing vicinal diols, which showed an antagonistic effect on bortezomib in this study, can be achieved through daily dietary intake: the *in vivo* plasma concentration of i.v.-injected bortezomib is 2 nM [57]; the *in vivo* plasma

concentration of catechin administered by 120 mL wine is 70 nM [56]; the *in vivo* plasma concentration of epicatechin administered by 600 mL cocoa is 100 nM [55]; and the *in vivo* plasma concentration of catechin administered by 600 mL cocoa is 300 nM [55]. In addition, many people consume polyphenols daily in the form of the herbal supplements or by drinking tea. For instance, the peak serum concentration of gallic acid at 2 h after drinking one cup of Assam black tea is approximately 2 μM, which is sufficiently high to show an inhibitory effect on an i.v.-injected anticancer agent, i.e., bortezomib [58]. One herbal supplement tablet also contains 25 mg of gallic acid, and a serum concentration of gallic acid as high as 1.8 μM can be attained by taking 2 tablets [58].

However, the concentrations of bortezomib (10 nM) and polyphenols (>50 μM) tested in this study may too high. We selected these concentrations in order to test various types of polyphenols and to present the results in the same figure as shown in Fig. 5A. In fact, we tested an RH up to 200 μM in MM cell lines to examine the maximum concentration as regards a blocking effect on 10 nM bortezomib. It showed no inhibitory effect at that concentration (data not shown). Thus, it remains unclear as to whether 200 μM of RH can or cannot inhibit the action of bortezomib due to the necessarily high concentration needed to determine this. In addition, although vicinal diols are a key factor in the blocking activity of bortezomib, this remains unclear in RH. RH, which is a derivative of QD, also has vicinal diols; RH did not show successful inhibitory activity like the other polyphenols. As shown in Fig. 3, RH has sugar in its chemical structure; this could decelerate the cell permeability and the blocking activity of bortezomib.

In this study, we used an *in vitro* cell-based format to determine the duration of the blocking effect of polyphenols. This could raise the questions regarding the effect of *in vivo* metabolism through the extensive biotransformation of dietary polyphenols including oxidation, reduction, methylation, sulfation, glucuronidation, *etc*. However, many of the *in vivo* researches noted above support the potential chemical interaction of polyphenols consumed through typical daily diets with bortezomib based on their structures [55-58]. The present results could help to establish crude guidelines suggesting that patients being treated with bortezomib should avoid the intake of herbal supplements or foods containing polyphenols in large quantities before clearance of bortezomib *in vivo*. In order to recommend specific guidelines for physicians, a study on the inhibitory effect of polyphenols and their metabolites on bortezomib in an *in vivo* system is currently underway. Since monotherapy of polyphenols *per se* showed strong antimyeloma activity, we recommend that polyphenols be consumed when the concentration of bortezomib is at its lowest point, such as between the injection cycles.

References

1. Barille-Nion S, Barlogie B, Bataille R, Bergsagel PL, Epstein J, Fenton RG, Jacobson J, Kuehl WM, Shaughnessy J, Tricot G: **Advances in biology and therapy of multiple myeloma**. *Hematology Am Soc Hematol Educ Program* 2003:248-278.
2. Hideshima T, Bergsagel PL, Kuehl WM, Anderson KC: **Advances in biology of multiple myeloma: clinical applications**. *Blood* 2004, **104**(3):607-618.
3. Cohen HJ, Crawford J, Rao MK, Pieper CF, Currie MS: **Racial differences in the prevalence of monoclonal gammopathy in a community-based sample of the elderly**. *Am J Med* 1998, **104**(5):439-444.
4. Hideshima T, Chauhan D, Richardson P, Anderson KC: **Identification and validation of novel therapeutic targets for multiple myeloma**. *Journal of clinical oncology : official journal of the American Society of Clinical Oncology* 2005, **23**(26):6345-6350.
5. Hideshima T, Anderson KC: **Molecular mechanisms of novel therapeutic approaches for multiple myeloma**. *Nat Rev Cancer* 2002, **2**(12):927-937.
6. Shaughnessy J, Jr., Gabrea A, Qi Y, Brents L, Zhan F, Tian E, Sawyer J, Barlogie B, Bergsagel PL, Kuehl M: **Cyclin D3 at 6p21 is dysregulated by recurrent chromosomal translocations to immunoglobulin loci in multiple myeloma**. *Blood* 2001, **98**(1):217-223.
7. Rasmussen T, Knudsen LM, Dahl IM, Johnsen HE: **C-MAF oncogene dysregulation in multiple myeloma: frequency and biological relevance**. *Leuk Lymphoma* 2003, **44**(10):1761-1766.
8. Fabris S, Agnelli L, Mattioli M, Baldini L, Ronchetti D, Morabito F, Verdelli D, Nobili L, Intini D, Callea V *et al*: **Characterization of oncogene dysregulation in multiple myeloma by combined FISH and**

DNA microarray analyses. *Genes Chromosomes Cancer* 2005, **42**(2):117-127.

9. Bommert K, Bargou RC, Stuhmer T: **Signalling and survival pathways in multiple myeloma**. *Eur J Cancer* 2006, **42**(11):1574-1580.
10. Anderson KC: **Clinical update: novel targets in multiple myeloma**. *Seminars in oncology* 2004, **31**(6 Suppl 16):27-32; discussion 33.
11. Koepp DM, Harper JW, Elledge SJ: **How the cyclin became a cyclin: regulated proteolysis in the cell cycle**. *Cell* 1999, **97**(4):431-434.
12. Ghosh S, May MJ, Kopp EB: **NF-kappa B and Rel proteins: evolutionarily conserved mediators of immune responses**. *Annual review of immunology* 1998, **16**:225-260.
13. Rock KL, Goldberg AL: **Degradation of cell proteins and the generation of MHC class I-presented peptides**. *Annual review of immunology* 1999, **17**:739-779.
14. Richardson PG, Barlogie B, Berenson J, Singhal S, Jagannath S, Irwin D, Rajkumar SV, Srkalovic G, Alsina M, Alexanian R *et al*: **A phase 2 study of bortezomib in relapsed, refractory myeloma**. *N Engl J Med* 2003, **348**(26):2609-2617.
15. Hideshima T, Richardson P, Chauhan D, Palombella VJ, Elliott PJ, Adams J, Anderson KC: **The proteasome inhibitor PS-341 inhibits growth, induces apoptosis, and overcomes drug resistance in human multiple myeloma cells**. *Cancer Res* 2001, **61**(7):3071-3076.
16. Cusack JC, Jr., Liu R, Houston M, Abendroth K, Elliott PJ, Adams J, Baldwin AS, Jr.: **Enhanced chemosensitivity to CPT-11 with proteasome inhibitor PS-341: implications for systemic nuclear factor-kappaB inhibition**. *Cancer Res* 2001, **61**(9):3535-3540.
17. LeBlanc R, Catley LP, Hideshima T, Lentzsch S, Mitsiades CS, Mitsiades N, Neuberg D, Goloubeva O, Pien CS, Adams J *et al*: **Proteasome inhibitor PS-341 inhibits human myeloma cell growth in vivo and prolongs survival in a murine model**. *Cancer Res* 2002, **62**(17):4996-5000.

18. Sanda T, Iida S, Ogura H, Asamitsu K, Murata T, Bacon KB, Ueda R, Okamoto T: **Growth inhibition of multiple myeloma cells by a novel IkappaB kinase inhibitor**. *Clin Cancer Res* 2005, **11**(5):1974-1982.

19. Miyakoshi S, Kami M, Yuji K, Matsumura T, Takatoku M, Sasaki M, Narimatsu H, Fujii T, Kawabata M, Taniguchi S *et al*: **Severe pulmonary complications in Japanese patients after bortezomib treatment for refractory multiple myeloma**. *Blood* 2006, **107**(9):3492-3494.

20. Hideshima T, Neri P, Tassone P, Yasui H, Ishitsuka K, Raje N, Chauhan D, Podar K, Mitsiades C, Dang L *et al*: **MLN120B, a novel IkappaB kinase beta inhibitor, blocks multiple myeloma cell growth in vitro and in vivo**. *Clin Cancer Res* 2006, **12**(19):5887-5894.

21. Surh YJ: **Cancer chemoprevention with dietary phytochemicals**. *Nat Rev Cancer* 2003, **3**(10):768-780.

22. Lee KW, Lee HJ: **The roles of polyphenols in cancer chemoprevention**. *Biofactors* 2006, **26**(2):105-121.

23. Beniston RG, Campo MS: **Quercetin elevates p27(Kip1) and arrests both primary and HPV16 E6/E7 transformed human keratinocytes in G1**. *Oncogene* 2003, **22**(35):5504-5514.

24. Russo M, Palumbo R, Mupo A, Tosto M, Iacomino G, Scognamiglio A, Tedesco I, Galano G, Russo GL: **Flavonoid quercetin sensitizes a CD95-resistant cell line to apoptosis by activating protein kinase Calpha**. *Oncogene* 2003, **22**(21):3330-3342.

25. Kuo PC, Liu HF, Chao JI: **Survivin and p53 modulate quercetin-induced cell growth inhibition and apoptosis in human lung carcinoma cells**. *J Biol Chem* 2004, **279**(53):55875-55885.

26. Park CH, Chang JY, Hahm ER, Park S, Kim HK, Yang CH: **Quercetin, a potent inhibitor against beta-catenin/Tcf signaling in SW480 colon cancer cells**. *Biochem Biophys Res Commun* 2005, **328**(1):227-234.

27. Alia M, Mateos R, Ramos S, Lecumberri E, Bravo L, Goya L: **Influence of quercetin and rutin on growth and antioxidant defense system of a human hepatoma cell line (HepG2)**. *Eur J Nutr* 2006, **45**(1):19-28.

28. Na HK, Surh YJ: **Intracellular signaling network as a prime chemopreventive target of (-)-epigallocatechin gallate**. *Mol Nutr Food Res* 2006, **50**(2):152-159.

29. Ogata S, Miyake Y, Yamamoto K, Okumura K, Taguchi H: **Apoptosis induced by the flavonoid from lemon fruit (Citrus limon BURM. f.) and its metabolites in HL-60 cells**. *Biosci Biotechnol Biochem* 2000, **64**(5):1075-1078.

30. Calcabrini A, Garcia-Martinez JM, Gonzalez L, Tendero MJ, Ortuno MT, Crateri P, Lopez-Rivas A, Arancia G, Gonzalez-Porque P, Martin-Perez J: **Inhibition of proliferation and induction of apoptosis in human breast cancer cells by lauryl gallate**. *Carcinogenesis* 2006, **27**(8):1699-1712.

31. Afaq F, Saleem M, Krueger CG, Reed JD, Mukhtar H: **Anthocyanin- and hydrolyzable tannin-rich pomegranate fruit extract modulates MAPK and NF-kappaB pathways and inhibits skin tumorigenesis in CD-1 mice**. *Int J Cancer* 2005, **113**(3):423-433.

32. Maria Russo RP, Annalisa Mupo, Mariarosaria Tosto, Giuseppe Iacomino,, Annamaria Scognamiglio IT, Giovanni Galano, and Gian Luigi Russo: **Flavonoid quercetin sensitizes a CD95-resistant cell line to apoptosis by activating protein kinase Ca**. 2003, **22**:3330-3342.

33. Chi Hoon Park JYC, Eun Ryeong Hahm, Seyeon Park,, Hyun-Kyung Kim CHY: **Quercetin, a potent inhibitor against b-catenin/Tcf signaling in SW480 colon cancer cells**. *Biochemical and Biophysical Research Communications* 2005, **328**:227-234.

34. Pao-Chen Kuo H-FL, and Jui-I Chao: **Survivin and p53 Modulate Quercetin-induced Cell Growth Inhibition and Apoptosis in Human Lung Carcinoma Cells**. *THE JOURNAL OF BIOLOGICAL CHEMISTRY* 2004, **279**:55875-55885.

35. Campo RGBaMS: **Quercetin elevates p27Kip1 and arrests both primary and HPV16 E6/E7 transformed human keratinocytes in G1**. 2003, **22**:5504-5514.

36. Mario Alía RM, Sonia Ramos, Elena Lecumberri, Laura Bravo, and Luis Goya: **Influence of quercetin and rutin on growth and antioxidant defense system of a human hepatoma cell line (HepG2)**. 2006, **45**:19-28.

37. Surh H-K, NaY-J: **intracellular signaling network as a prime chemopreventive target of (-)-epigallocatechin gallate**. *Mol Nurt Food Res* 2006, **50**:152-159.

38. Shin Ogata YM, Kanefumi Yamamoto, Katsuzumi Okumura, and Hiroshi Taguchi: **Apoptosis induced by the flavonoids from lemon fruit (Citrus limon BURM. f.) and its metabolites in HL-60 cells**. *Biosci Biotechnol Biochem* 2000, **64**:1075-1078.

39. Calcabrini A G-MJ, González L, Tendero MJ, Ortuño MT, Crateri P, Lopez-Rivas A, Arancia G, González-Porqué P, Martín-Pérez J: **Inhibition of proliferation and induction of apoptosis in human breast cancer cells by lauryl gallate**. *Carcinogenesis* 2006, **27**:1699-1712.

40. Farrukh Afaq MS, Christian G. Krueger, Jess D. Reed and Hasan Mukhtar: **Anthocyanin- and Hydrolyzable Tannin-Rich Pomegranate Fruit Extract Modulates MAPK and NF- B Pathways and Inhibits Skin Tumorigenesis in CD-1 Mice**. *Int J Cancer* 2005, **113**:423-433.

41. Dai Y, Rahmani M, Pei XY, Dent P, Grant S: **Bortezomib and flavopiridol interact synergistically to induce apoptosis in chronic myeloid leukemia cells resistant to imatinib mesylate through both Bcr/Abl-dependent and -independent mechanisms**. *Blood* 2004, **104**(2):509-518.

42. Hideshima T, Bradner JE, Wong J, Chauhan D, Richardson P, Schreiber SL, Anderson KC: **Small-molecule inhibition of proteasome and aggresome function induces synergistic antitumor activity in multiple myeloma**. *Proc Natl Acad Sci U S A* 2005, **102**(24):8567-8572.

43. Chauhan D, Singh A, Brahmandam M, Podar K, Hideshima T, Richardson P, Munshi N, Palladino MA, Anderson KC: **Combination of proteasome inhibitors bortezomib and NPI-0052 trigger in vivo synergistic cytotoxicity in multiple myeloma**. *Blood* 2008, **111**(3):1654-1664.

44. Fernandez Y, Miller TP, Denoyelle C, Esteban JA, Tang WH, Bengston AL, Soengas MS: **Chemical blockage of the proteasome inhibitory function of bortezomib: impact on tumor cell death**. *J Biol Chem* 2006, **281**(2):1107-1118.

45. Zou W, Yue P, Lin N, He M, Zhou Z, Lonial S, Khuri FR, Wang B, Sun SY: **Vitamin C inactivates the proteasome inhibitor PS-341 in human cancer cells**. *Clin Cancer Res* 2006, **12**(1):273-280.

46. Liu FT, Agrawal SG, Movasaghi Z, Wyatt PB, Rehman IU, Gribben JG, Newland AC, Jia L: **Dietary flavonoids inhibit the anticancer effects of the proteasome inhibitor bortezomib**. *Blood* 2008, **112**(9):3835-3846.

47. Bongiorno RA, Nutescu EA: **Generic warfarin: implications for clinical practice and perceptions of anticoagulation providers**. *Semin Thromb Hemost* 2004, **30**(6):619-626.

48. MARIA J. CHEN PPC, BIH-YING YANG, HUNG CHIEH LO, JIN-KI SON, JERRY HENDRICKS, GEORGE BAILEY, and THOMAS T. CHEN: **DEVELOPMENT OF RAINBOW TROUT HEPATOMA CELL LINES: EFFECT OF PRO-IGF-I EA4-PEPTIDE ON MORPHOLOGICAL CHANGES AND ANCHORAGE-INDEPENDENT GROWTH**. *In Vitro Cellular & Developmental Biology - Animal* 2004, **40**:118–128

49. Wong IH, Ng MH, Huang DP, Lee JC: **Aberrant p15 promoter methylation in adult and childhood acute leukemias of nearly all morphologic subtypes: potential prognostic implications**. *Blood* 2000, **95**(6):1942-1949.

50. Miller CP, Ban K, Dujka ME, McConkey DJ, Munsell M, Palladino M, Chandra J: **NPI-0052, a novel proteasome inhibitor, induces caspase-8 and ROS-dependent apoptosis alone and in combination with HDAC inhibitors in leukemia cells**. *Blood* 2007, **110**(1):267-277.

51. Adams J: **The proteasome: a suitable antineoplastic target**. *Nat Rev Cancer* 2004, **4**(5):349-360.

52. Landis-Piwowar KR, Milacic V, Chen D, Yang H, Zhao Y, Chan TH, Yan B, Dou QP: **The proteasome as a potential target for novel anticancer drugs and chemosensitizers**. *Drug Resist Updat* 2006, **9**(6):263-273.

53. Norrild JC: **An illusive chiral aminoalkylferroceneboronic acid. Structural assignment of a strong 1:1 sorbitol complex and new insight into boronate-polyol interactions**. *Journal of the Chemical Society Perkin Transactions* 2001, **2**:719-726.

54. Gao X, Zhang Y, Wang B: **New boronic acid fluorescent reporter compounds. 2. A naphthalene-based on-off sensor functional at physiological pH**. *Org Lett* 2003, **5**(24):4615-4618.

55. Schroeter H, Heiss C, Balzer J, Kleinbongard P, Keen CL, Hollenberg NK, Sies H, Kwik-Uribe C, Schmitz HH, Kelm M: **(-)-Epicatechin mediates beneficial effects of flavanol-rich cocoa on vascular function in humans**. *Proc Natl Acad Sci U S A* 2006, **103**(4):1024-1029.

56. Donovan JL, Bell JR, Kasim-Karakas S, German JB, Walzem RL, Hansen RJ, Waterhouse AL: **Catechin is present as metabolites in human plasma after consumption of red wine**. *J Nutr* 1999, **129**(9):1662-1668.

57. Ogawa Y, Tobinai K, Ogura M, Ando K, Tsuchiya T, Kobayashi Y, Watanabe T, Maruyama D, Morishima Y, Kagami Y *et al*: **Phase I and II pharmacokinetic and pharmacodynamic study of the proteasome inhibitor bortezomib in Japanese patients with relapsed or refractory multiple myeloma**. *Cancer Sci* 2008, **99**(1):140-144.

58. Shahrzad S, Aoyagi K, Winter A, Koyama A, Bitsch I: **Pharmacokinetics of gallic acid and its relative bioavailability from tea in healthy humans**. *J Nutr* 2001, **131**(4):1207-1210.

국문 초록

金 兌 映

다발골수종 (multiple myeloma)은 골수 내 형질세포의 악성 증식에 의해 발생하는 혈액암의 일종이다. 보르테조밉 (bortezomib)은 다발골수종 치료제로 사용된 최초의 프로테아좀 (proteasome) 억제제이며, 폴리페놀 (polyphenols)은 암에서 항세포증식 효과를 보이는 것으로 잘 알려진 물질이다. 우리는 복합약제효과를 관찰하기 위해 세가지 골수종세포주 (U266, RPMI8226, MC/CAR)에 보르테조밉과 함께 여섯 종류의 폴리페놀 (rutin, quercetin, caffeic acid, gallic acid, EGCG, tannic acid)을 농도를 달리하면서 동시에 처리하였다. 그러나, 보르테조밉의 항암효과는 정도의 차이는 있었으나 폴리페놀에 의해 억제되었으며, 다발골수종 환자로부터 분리한 CD138+ 일차 골수종 세포에서도 동일한 결과를 관찰하였다. 폴리페놀의 구조적 특징이 보르테조밉과의 길항효과와 연관이 있음을 관찰하였는데, 특히 비시날 다이올 (vicinal diol) 부분의 존재 여부가 보르테조밉의 항암 기능을 억제하는 주요 인자였다. 우리는 폴리페놀의 비시날 다이올이 보르테조밉의 보론산 (boronic acid)과 작용하여 보르테조밉의 활성 삼각구조를 불활성 사면체 보로네이트 (boronate)로 바꾸어, 이것이 보르테조밉의 골수종 항암효과를 상쇄시키는 것이라

추론하였다. 이러한 가설을 보르테조밉과 EGCG 간의 ^{11}B 핵자기공명 (nuclear magnetic resonance spectroscopy) 실험을 통해 확인하였다. 이러한 결과들에 근거하여, 음식이나 비타민 보조제에 자연적으로 존재하는 폴리페놀을 섭취하는 것이 보르테조밉을 처방 받은 다발골수종 환자들에서는 검토되어야만 하겠다.

주요어 : 보르테조밉, 폴리페놀, 다발골수종, 약물간 상호반응, 비시날 다이올

학번: 2005-30677